CrossMark

Measurements of natural gamma radiation in beach sediments of north east coast of Tamilnadu, India by gamma ray spectrometry with multivariate statistical approach

M. SureshGandhi [a], **R. Ravisankar** [b,*], **A. Rajalakshmi** [c], **S. Sivakumar** [d], **A. Chandrasekaran** [e], **D. Pream Anand** [f]

[a] Department of Geology, University of Madras, Guindy Campus, Chennai 600 025, Tamilnadu, India
[b] Post Graduate and Research Department of Physics, Government Arts College, Tiruvannamalai 606603, Tamilnadu, India
[c] Department of Physics, SSN College of Engineering, Kalavakkam, Chennai 603 110, Tamil Nadu, India
[d] Department of Physics, Mailam Engineering College, Mailam 604304, Tamilnadu, India
[e] Department of Physics, Global Institute of Engineering & Technology, Vellore 632509, Tamilnadu, India
[f] Department of Physics, ST. XAVIER'S College, Palayamkottai 627002, Tamilnadu, India

ARTICLE INFO

ABSTRACT

The distribution of natural gamma ray emitting ^{238}U, ^{232}Th and ^{40}K radionuclides in beach sediments along north east coast of Tamilnadu, India has been carried out using a NaI(Tl) gamma ray spectrometric technique. The total average concentrations of radionuclides ^{238}U, ^{232}Th, and ^{40}K were 35.12, 713.16, and 349.60 Bq kg^{-1}, respectively. Correlations made among these radionuclides prove the existence of secular equilibrium in the investigated sediments. The total average absorbed dose rate in the study areas is found to be 504.75 nGyh^{-1}, whereas the annual effective dose rate has an average value of 0.62 mSvy^{-1}. The mean activity concentrations of measured radionuclides were compared with other literature values. The ratios between the detected radioisotopes have been calculated for spatial distribution of natural radionuclides in studied area. Also the radiological hazard of the natural radionuclides content, radium equivalent activity, external hazard index of the sediment samples in the area under consideration were calculated. Multivariate Statistical analyses (Pearson Correlation, Cluster and Factor analysis) were carried out between the parameters obtained from radioactivity to know the existing relations.

Copyright © 2014, The Egyptian Society of Radiation Sciences and Applications. Production and hosting by Elsevier B.V. All rights reserved.

* Corresponding author. Tel.: +91 9443520354; fax: +91 4175 236553.
  E-mail address: ravisankarphysics@gmail.com (R. Ravisankar).

Production and hosting by Elsevier

1.   Introduction

All living organisms of the planet are exposed to natural radiation, which is mainly due to the activity concentration of primordial radionuclides ^{232}Th, ^{238}U and their product of decay, in addition to the other natural radionuclide ^{40}K present in the earths crust (UNSCEAR, 2000). Natural radioactivity is wide spread in the earth's environment and it exists in various geological formations like soils, rocks, plants, sand, water and air. Hence, humans should beware of their natural environment with regard to the radiation health effects. Some of the radiation health effects are chronic lung diseases, acute leucopoenia, anemia and necrosis of the mouth. Thorium exposure can cause lung, pancreas, hepatic, bone, kidney cancers and leukemia (Taskin et al., 2009). Therefore nowadays, human exposure to ionizing radiation is one of the scientific subjects that attracts public attention, since radiation of natural origin is responsible for most of the total radiation exposure of the human population. Many areas in the world such as Australia, Brazil, China, India, Iran, Japan, etc., possess high levels of natural radiation. In the recent years, studies on the high background radiation areas in the world have been of prime importance for risk estimation due to long term low-level whole body exposures to the public. The high radiation levels are due to the presence of large quantities of naturally occurring radioactive minerals in the rocks, soils, sediments, etc. (Singh, Shanker, Neelakandan, & Singh, 2007). Among the various geological formations, sediment plays a predominant role in aquatic radioecology and plays a role in accumulating and transporting contaminants within the geographic area. It is the basic indicator of radiological contamination in the environment (Suresh, Ramasamy, Meenakshisundaram, Venkatachalapathy, & Ponnusamy, 2011).

Sediment is a naturally occurring material that is broken down by processes of weathering and erosion, and is subsequently transported by the action of wind, water, or ice, and/or by the force of gravity acting on the particle itself. Sediments are most often transported by water (fluvial processes), wind (aeolian processes) and glaciers. Beach sands and river channel deposits are examples of fluvial transport and deposition, though sediment also often settles out of slow-moving or standing water in lakes and ocean dunes and loess are examples of aeolian transport and deposition. Glacial moraine deposits and till are ice-transported sediments. Seas, oceans and lakes accumulate sediment over time. The sediment could consist of terrigenous material, which originates on land, but may be deposited in either terrestrial, marine, or lacustrine (lake) environments; or of sediments (often biological) originating in the body of water. Terrigenous material is often supplied by nearby rivers and streams or reworked marine sediment (e.g. sand). In the mid-ocean, living organisms are primarily responsible for the sediment accumulation, their shells sinking to the ocean floor upon death. Deposited sediments are the source of sedimentary rocks, which can contain fossils of the inhabitants of the body of water that were, upon death, covered by accumulating sediment. Lake bed sediments that have not solidified into rock can be used to determine past climatic conditions.

Beach sediments are mineral deposits formed through weathering and erosion of either igneous or metamorphic rocks. Among the rock constituent minerals are some natural radionuclides that contribute to ionizing radiation exposure on Earth. Natural radioactivity in soils comes from U and Th series and natural K. The study of the distribution of primordial radionuclides allows the understanding of the radiological implication of these elements due to the gamma-ray exposure of the body and irradiation of lung tissue from inhalation of radon and its daughters (Uosif, El-Taher, & Abbady, 2008). Radiological studies have been made in sediment beach locations, mainly in India, because along its coastline there are quite a few monazite sand bearing placer deposits causing natural high background radiation areas in Kerala (UNSCEAR, 2000) and Tamilnadu (Radhakrishna, Somashekarappa, Narayana, & Siddappa, 1993), in Kalpakkam (Kannan, Rajan, Iyengar, & Ramesh, 2002) and in recent work in the coast of Orissa (Mohanty, Sengupta, Das, Vijayan, & Saha, 2004). During the last few decades, the coastal environment of north east coast of Tamilnadu in India has experienced intense developments in industry, tourism, transport, urbanization and aquaculture. This paper reports the activity concentrations of natural radionuclides ^{238}U, ^{232}Th and ^{40}K, for beach sediments of north east coast of Tamilnadu, India.

The objective of this paper is to evaluate the radiological hazards due to natural radioactivity associated with beach sediments by calculating the radium equivalent activity (R_{eq}), absorbed dose rate (D_R), annual effective dose rate (AEDR) and External hazard index (H_{ex}). The data generated in this study may contribute to the natural radioactivity level database for this area and multivariate statistical techniques were applied to know the relationship between radionuclide and radiological parameters.

2.   Materials and methods

2.1.   Study area

The present study area covers from Besant Nagar (longitude 80.2668E and latitude13.0002N) to Aliyakuppam (longitude79.814722200E and latitude 11.890833300N) of Pondicherry city about 165 km. Fig. 1 shows the collected sample locations. The present study area covers many industries, most famous tourism place and nuclear power plant. The sample location were recorded in terms of degree - minute - second (Latitudinal and Longitudinal position) using handheld Global Positioning System (GPS) (Model: GARMIN GPS-12) unit. Each location is separated by a distance of 10—15 km approximately.

2.2.   Sample collection

Sediment samples were collected using Peterson grab at all the designated locations during low tide. The sediment sample was collected from a depth of 5 cm from the surface. Each sample has the weight of about 3 kg. The collected samples were air dried at room temperature in open air. The samples were placed in plastic pouches and transported to the laboratory.
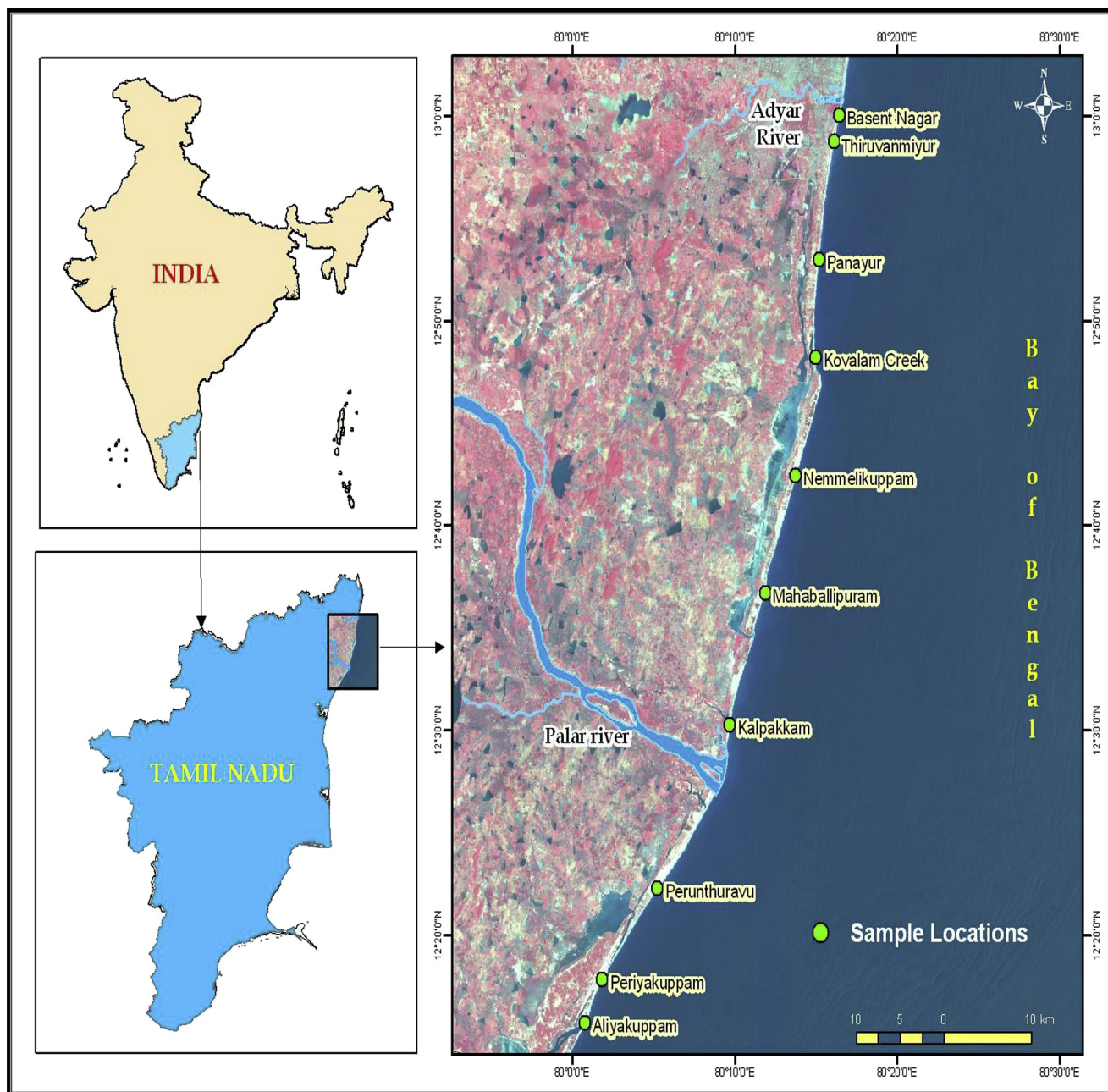
Fig. 1 — Sample collected locations of north east coast of Tamilnadu.

2.3. Sample preparation

The collected samples were dried in an oven at $100-110\ ^\circ C$ for about 24 h and sieved through a 2 mm mesh-size sieve to remove stone, pebbles and other macro-impurities. The homogenized sample was placed in a 250 g airtight PVC container. The inner lid was placed in and closed tightly with outer cap. The container was sealed hermetically and externally using cellophane tape and kept aside for about a month to ensure equilibrium between ^{226}Ra and its daughter products before being taken for gamma ray spectrometric analysis (Ramasamy, Murugesan, & Mullainathan, 2004).

2.4. Gamma ray spectrometric analysis

All samples were subjected to gamma spectral analysis with a counting time of 10,000 s. A $3'' \times 3''$ NaI (Tl) detector was employed with adequate lead shielding which reduced the background by a factor of about 95%. The concentrations of various radionuclides of interest were determined in Bq kg^{-1} using the count spectra. The gamma-ray photo peaks corresponding to 1.46 MeV (^{40}K), 1.76 MeV (^{214}Bi) and 2.614 MeV (^{208}Tl) were considered in arriving at the activity of ^{40}K, ^{238}U and ^{232}Th in the samples. The detection limit of NaI(Tl) detector system for ^{40}K, ^{238}U and ^{232}Th are 8.5, 2.21

Table 1 – Activity concentration, radium equivalent (Ra$_{eq}$), absorbed dose rate (D_R), annual effective dose rate (H_R), external hazard index (H_{ex}).

S. no	Location	Activity concentration (Bq Kg^{-1})			Ra$_{eq}$	Absorbed dose rate (D_R) (nGyh^{-1})	Annual effective dose rate (mSvy^{-1})	H_{ex}
		^{238}U	^{232}Th	^{40}K				
1	Besant Nagar	33.58	259.14	260.5	424.21	197.97	0.244	1.145
2	Thiruvanmiyur	15.89	113.26	299.57	200.92	94.85	0.117	0.543
3	Payanurkuppam (AVM Studio)	30.24	461.57	317.03	714.70	333.72	0.410	1.930
4	Kovalam Creek (Estuary)	BDL	106.74	393.04	182.90	87.60	0.108	0.494
5	Nemilikuppam	104.6	2139.57	306.03	3187.75	1482.78	1.824	8.607
6	Mahabalipuram	96.83	2856.82	560.43	4225.24	1967.82	2.420	11.408
7	Kalpakkam	33.29	519.41	396.28	806.56	376.89	0.464	2.178
8	Periyakuppam	BDL	24.35	318.38	59.34	29.59	0.036	0.160
9	Perumthuravu	17.83	494.47	393.95	755.26	353.53	0.435	2.039
10	Marakanam (Estuary)	18.99	156.27	250.87	261.77	122.78	0.151	0.707
Average		35.12	713.16	349.60	1081.86	504.75	0.621	2.921

and 2.11 Bq kg^{-1} respectively for a counting time of 10,000 s.

2.5. Statistical analysis

The method of univariate statistics was applied to process the analytical data in terms of its distribution and correlation between pairs of studied parameters. Some of the basic parameters included in this study are given in Table 1. The multivariate statistics involving PCA and CA were used to determine the origin of elements studied in sediment samples. This latter analysis was duly supported by the univariate statistics and linear regression relationships. The data were processed by the Varimx normalized method for the evaluation of PCA. SPSS.16.0 software was used to conduct the relevant statistical analysis of the data.

3. Results and discussions

3.1. Activity concentrations of ^{238}U, ^{232}Th and ^{40}K in the sediments

The activity concentrations of ^{238}U, ^{232}Th and ^{40}K sediment samples are given in Table 1. All values are given in Bq kg^{-1} of dry weight. The activities range and mean values (in brackets) for ^{238}U, ^{232}Th and ^{40}K are ≤2.21−104.6 (35.12), 24.35−2856.82 (713.16) and 250.9−560.4 (349.60) Bq kg^{-1}, respectively. The

wide variations of the activity concentration values are due to their presence in the marine environment and their physical, chemical and geo-chemical properties (El Mamoney & Khater, 2004; Khatir, Ahamed, El-Khangi, Nigumi, & Holm, 1998). The results show that the mean activity of ^{238}U and ^{232}Th and is higher when compared with worldwide average value (35 Bq kg^{-1} for ^{238}U, 30 Bq kg^{-1} for ^{232}Th and 400 Bq kg^{-1} for ^{40}K) of this radionuclide in the sediment (UNSCEAR, 2000). Table 2 compares the activity concentrations of ^{238}U, ^{232}Th and ^{40}K in beach sediment samples of north east coast of Tamilnadu, India and other studies in different beaches of the world.

The maximum activity concentration of ^{40}K was observed in Mahabalipuram which is one of the famous historical and tourism place. The highest activity concentration of ^{238}U was found in Nemilikuppam nearer to Chennai metro city. The lowest concentration of ^{238}U was found at Perumthuravu (17.83 Bq Kg^{-1}), Marakanam (18.99 Bq Kg^{-1}) which are near to Pudhucherry beach which may be due to high composition of Si. Fig. 2 shows the variation of activity concentration at different sampling locations.

3.2. Radium equivalent activity concentration index (Ra$_{eq}$)

The radium equivalent activity concentration index, Ra$_{eq}$ (Mahur, Kumar, Sonkawade, Sengupta, & Prasad, 2008) was calculated according to Eq. (1). The radium equivalent concept

Table 2 – Comparison of activity concentrations of ^{238}U, ^{232}Th and ^{40}K in beach sediment samples of North east coast of Tamilnadu, India and other studies in different beaches of the world.

| S. no	Locations	^{238}U (Bq Kg^{-1})	^{232}Th (Bq Kg^{-1})	^{40}K (Bq Kg^{-1})	References
1	World	35	30	400	UNSCEAR (2000)
2	India	28.67	63.83	327.6	UNSCEAR (2000)
3	Beach sand Egypt	−	177	815	Uosif et al. (2008)
4	Beach sand Red sea coast Egypt	23.1	7.2	338	Harb (2008)
5	Hungary	28.67	27.96	302.4	UNSCEAR (2000)
6	Kuwait	36	6	227	Saad & Al-Azmi (2002)
7	Nigeria	16	24	35	Arogunjo, Farai, & Fuwape (2004)
8	Kalpakkam in Tamilnadu, India	112	1455.8	351	Kannan et al. (2002)
9	Ullal in Karnataka, India	374	158	158	Radhakrishna et al. (1993)
10	North east coast of Tamilnadu , India	35.12	713.6	349.6	Present study
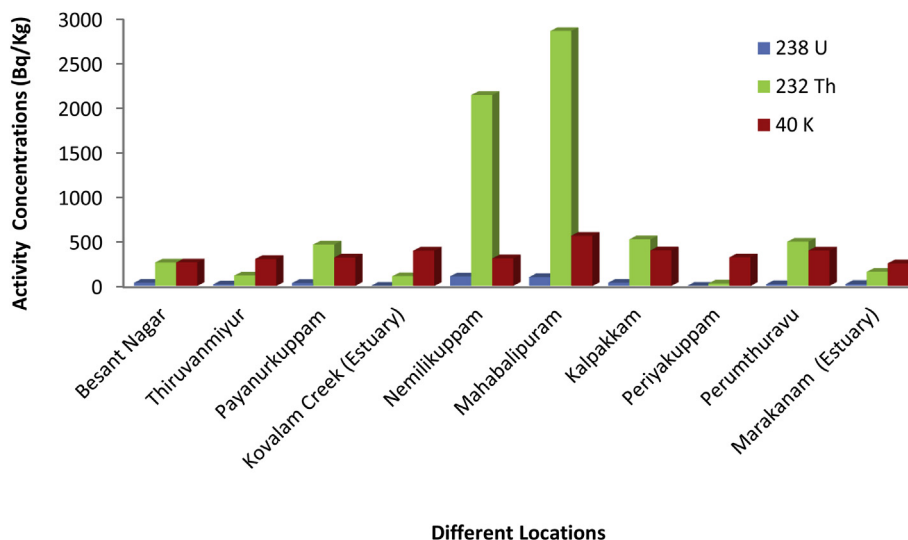
Fig. 2 – Variation of activity concentration at different sampling locations.

allows a single index or number to describe the gamma output from different mixtures of uranium, thorium, and ^{40}K in sediments samples from different locations.

$$Ra_{eq} = A_U + 1.43A_{Th} + 0.07A_K \tag{1}$$

where A_U, A_{Th} and A_K are the activity concentrations of ^{238}U, ^{232}Th and ^{40}K (Bq kg^{-1}), respectively. It has been assumed here that 370 Bq kg^{-1} of ^{238}U or 259 Bq kg^{-1} of ^{232}Th or 4810 Bq kg^{-1} of ^{40}K produce the same gamma dose rate. Ra_{eq} is related to the external γ-dose and internal dose due to radon and its daughters.

As can be seen from Table 1, the Ra_{eq} values for the sediment samples varied from 53.34 to 4225.54 Bq kg^{-1} with the average of 1081.86 Bq kg^{-1}. It is noteworthy that expect 4 locations the values of Ra_{eq} values are exceeds the suggested maximal admissible value of 370 Bq kg^{-1} (Beretka & Matthew, 1985). Fig. 3 shows the locations and radium equivalent activity (Ra_{eq}).

3.3. Evaluation of radiological hazard effects

3.3.1. Absorbed gamma dose rate
The absorbed gamma dose rates due to gamma radiations in air at 1 m above the ground surface for the uniform distribution of the naturally occurring radionuclides (^{238}U, ^{232}Th and ^{40}K) were calculated based on guidelines provided (UNSCEAR, 2000). The conversion factors used to compute absorbed gamma dose rate (D_R) in air per unit activity concentration in Bq kg^{-1} (dry weight) corresponds to 0.462 nGyh^{-1} for ^{238}U, 0.604 nGyh^{-1} for ^{232}Th and 0.042 nGyh^{-1} for ^{40}K. Therefore D_R can be calculated as follows (UNSCEAR, 2000),

$$D_R(nGyh^{-1}) = 0.462A_U + 0.604A_{Th} + 0.042A_K \tag{2}$$

where A_U, A_{Th} and A_K are the activity concentrations of ^{238}U, ^{232}Th and ^{40}K in Bq kg^{-1}, respectively. The absorbed dose rate values ranged between 29.59 and 1967.82, with a mean value of
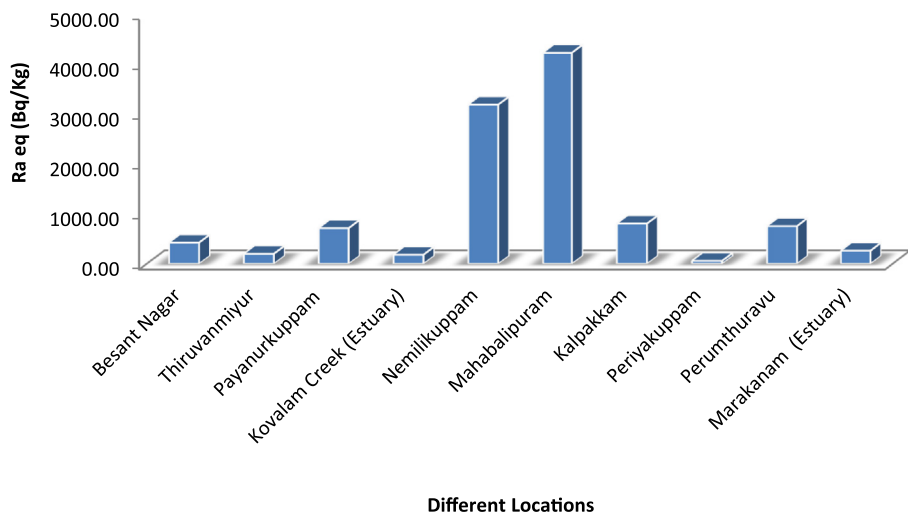

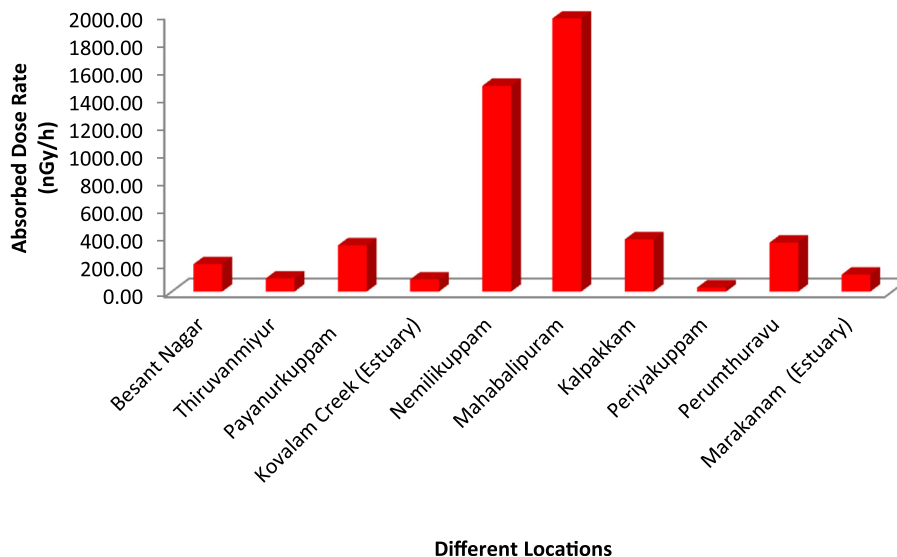**Fig. 3 – Locations and radium equivalent activity (Ra_{eq}).**

Fig. 4 − Variation of absorbed gamma dose rate with different locations.

504.75 nGyh^{-1}. The estimated mean value of D_R in the studied samples is higher than the world average (populated-weighted) absorbed gamma dose rate of 84 nGyh^{-1}. This may be due to high content of monazite deposits in the locations. Fig. 4 shows the variation of absorbed gamma dose rate with different locations.

3.3.2. Annual effective dose rate

The annual effective dose rate in mSvy^{-1} was calculated by the following formula (UNSCEAR, 2000),

$$H_R = D_R\left(nGyh^{-1}\right) \times 8760 \, h \times 0.2 \times 0.7 SvGy^{-1} \times 10^{-6} \quad (3)$$

The calculated AEDR values are ranged from 0.036 to 2.42 mSvy^{-1} with a mean value of 0.621 mSvy^{-1}, which is greater than the world average value of 0.07 mSvy^{-1} [1]. Highest value is observed at Mahabalipuram (2.42 mSvy^{-1}), which is

34.5 times higher than recommended level. In present study all the locations where the outdoor AEDR are not exceed the world average. It is due to the presence of low activity concentration of radionuclides. Fig. 5 show the variation of indoor effective dose with different locations.

3.3.3. External hazard index (H_{ex})

In order to assess the health effects from the radio activity of the earth's surface materials containing ^{238}U, ^{232}Th and ^{40}K, the activity of these nuclides is converted into a single quantity termed as external hazard index (H_{ex}). The prime objective of this index is to limit the radiation dose to dose equivalent limit of 1 mSvy^{-1} (ICRP, 1992). H_{ex} must not exceed the limit of unity for the radiation hazard to be negligible. Gamma Index deals with the assessment of excess gamma radiation
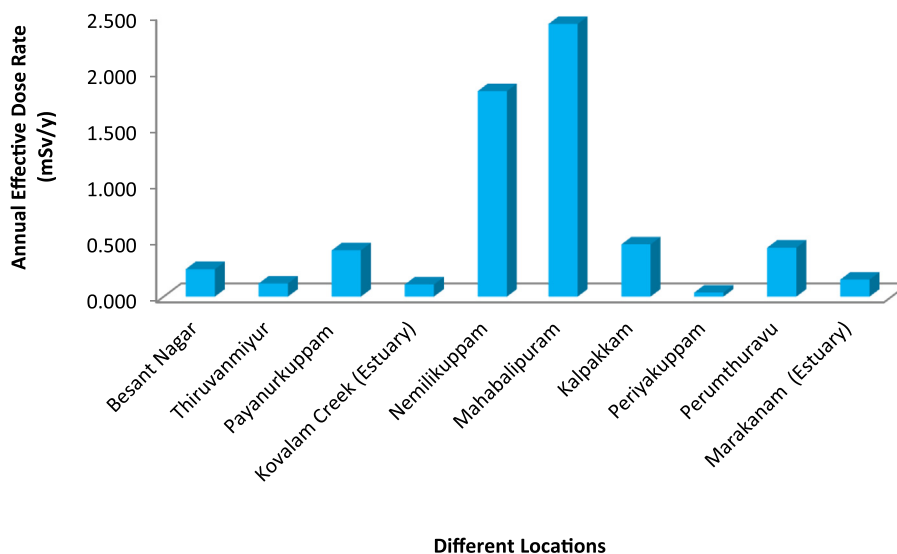

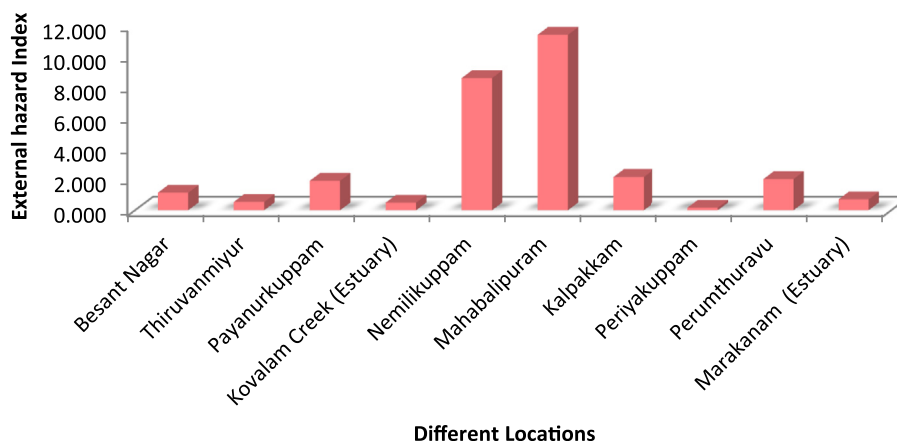**Fig. 5 − Variation of annual effective dose rate with different locations.**

Fig. 6 – Sample locations with variation of external hazard index.

originating from the present sediments. The external hazard index (H_{ex}) can then be defined as

$$H_{ex} = \frac{A_U}{370 Bq/Kg} + \frac{A_{Th}}{259 Bq/Kg} + \frac{A_K}{4810 Bq/Kg} \qquad (4)$$

where A_U, A_{Th}, and A_K are the activity concentrations of ^{238}U, ^{232}Th and ^{40}K, respectively. This index value must be less than unity in order to keep the radiation hazard to be insignificant. The calculated external hazard values are between 0.543 and 11.408 (Table 1). The mean value of the external hazard index (2.921) is greater than the recommended limit. Six locations such as Besant Nagar, Payanurkuppam, Nemilikuppam, Mahabalipuram, Kalpakkam and Perumthuravu exceeds the recommended limit. Exceedance of the recommended upper limit is noted in these locations. This exceedance in these sites is due to the higher concentration of radionuclides. Here also, average relative contribution to the gamma-index due to the ^{232}Th is higher followed by the contributions due to ^{40}K and ^{238}U. Fig. 6 shows sample locations with variation of external hazard index.

4. Multivariate statistical analysis

Conventional and multivariate statistical procedures for data treatment and histograms were performed using the commercial statistics software package SPSS version 16.0 for Windows. Cluster analysis and Pearson correlation were carried out in order to clarify the relationship among the variables, especially the influence of sediment radiological parameters on the distribution of natural radionuclides. Cluster analysis is a useful statistical method which presents visually the degree of association among variables. The distance axis displays the degree of association between groups of variables, i.e., the lower the value on the axis, the more significant the correlation (Facchinelli, Sacchi, & Mallen, 2001).

Principal components analysis (PCA) is the most common technique used to summarize patterns among variables in multivariate datasets. The PCA is a way of identifying patterns in variables, and expressing data in such a way as to highlight their similarities and differences The main advantage of PCA is that, once the patterns have been found, data can be compressed reducing the number of dimensions, without much loss of information.

4.1. Basic statistics

Statistical behavior of the measured data is presented in Table 3, which includes the range (minimum–maximum), arithmetic mean (AM), arithmetic standard deviation (SD), median, mode, skewness, kurtosis and the type of frequency distribution for the three radionuclides for all the sediment samples. The basic statistics show that the AM of activity concentrations are different from each other but are close within the SD. The precipitation affects the natural radioactivity of the soils, when rain water mixes with SO_2 of the air, then rain become acidic. Acid rain causes accelerated mobilization of many materials in sediments, especially ^{238}U (Sheppard & Sheppard, 1988).

In Probability theory and Statistics, Skewness is a measure of the asymmetry of the probability distribution of a real valued random variable. Skewness has benefits in many areas. Many models assume normal distribution; i.e., data are symmetric about the mean. The normal distribution has a Skewness of zero. However, in reality, data points may not be perfectly symmetric. Therefore, an understanding of the Skewness of the dataset indicates whether deviations from the mean are going to be positive or negative. Skewness characterizes the degree of asymmetry of a distribution

Table 3 – Descriptive statistics of radiological parameters.

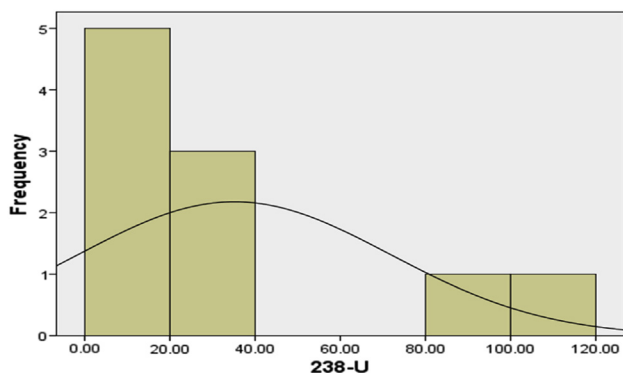| Variables	^{238}U	^{232}Th	^{40}K
Mean (AM)	35.125	713.16	349.608
Median	24.615	360	317.705
Std. Deviation (SD)	36.60	972	91.0467
Variance	1340	944100	8290
Skewness	1.322	1.77	1.417
Kurtosis	0.66	2.001	2.514
Minimum	BDL	24.35	250.9
Maximum	104.6	2856.82	560.4
Frequency distribution	Log-normal	Log-normal	Log-normal

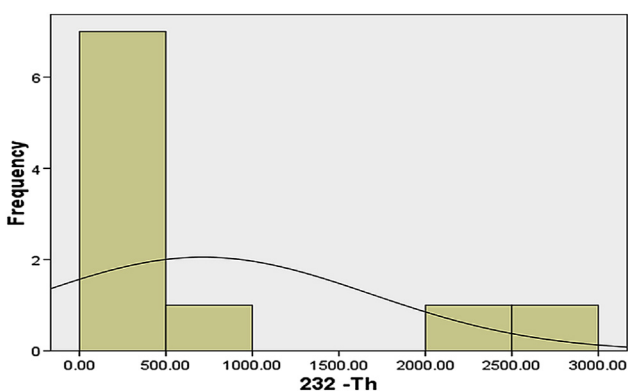**Fig. 7 — Frequency distribution of ^{238}U.**

Fig. 8 — Frequency distribution of ^{232}K.
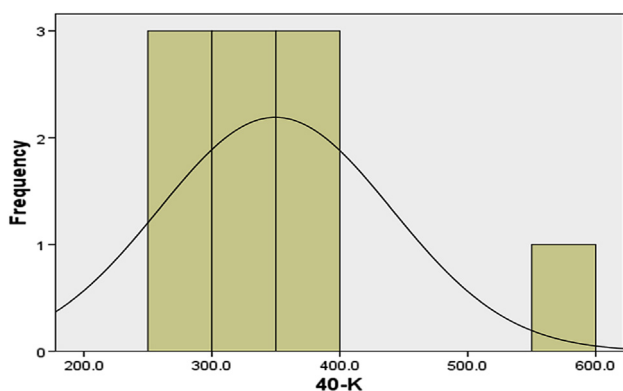

Fig. 9 — Frequency distribution of ^{40}K.

around its mean (Groeneveld & Meeden, 1984). Positive Skewness indicates a distribution with an asymmetric tail extending towards values that are more positive. Negative Skewness indicates a distribution with an asymmetric tail extending towards values that are more negative. Lower Skewness value form generally normal distributions. All the radionuclides have the Positive Skewness values (Table 2) which indicates asymmetric distribution.

Kurtosis is a measure of the peakedness of the probability distribution of a real-valued random variable. It characterizes the relative peakedness or flatness of a distribution compared with the normal distribution. Positive Kurtosis indicates a relatively peaked distribution. Negative Kurtosis indicates a relatively flat distribution. Higher Kurtosis means more of the variance is the result of infrequent extreme deviations, as opposed to frequent modestly sized deviations. In the present case ^{238}U, ^{40}K and ^{232}Th have a positive Kurtosis which indicates relatively peaked distribution (Table 2).

4.2. Histograms

In statistics, a histogram is a graphical representation of the distribution of data. It is an estimate of the probability distribution of a continuous variables. The frequency distribution for all radioactive variables in sediments samples were analyzed, where the histograms are given in Figs. 7−9. The graph of ^{40}K shows that these radionuclides demonstrate a normal (bell-shape) distribution. But ^{238}U and ^{232}Th exhibited some degree of multi-modality. This multi-modal feature of the radio elements demonstrates the complexity of minerals in sediment samples.

4.3. Pearson's correlation coefficient analysis

Correlation analysis has been carried out, as a bivariation statistics in order to determine the mutual relationships and strength of association between pairs of variables through calculation of the linear Pearson correlation coefficient. Results for Pearson correlation coefficients between all the studied radioactive variables for sediments are shown in Table 4.

The high good positive correlation co-efficient was absorbed between ^{232}Th and ^{226}Ra because radium and thorium decay series occurs together in nature (Tanaskovic, Golobocanin, & Miljevic, 2012). The positive correlation co-efficient was absorbed between ^{238}U, ^{232}Th and ^{40}K with all the radiological parameters. This implies that very strong relationship between the radionuclides in sediments and

Table 4 — Pearson correlation coefficients between radioactive variables in sediment samples.

Variables	^{238}U	^{232}Th	^{40}K	Ra_{eq}	D_R	AEDR	H_{ex}
^{238}U	1						
^{232}Th	0.948	1					
^{40}K	0.385	0.628	1				
Ra_{eq}	0.950	0.999	0.625	1			
D_R	0.949	0.999	0.626	0.999	1		
AEDR	0.949	0.999	0.626	0.999	0.999	1	
H_{ex}	0.950	0.999	0.625	0.999	0.999	0.999	1

Table 5 — Roated factor loadings of factor-1 & factor-2.

Variables	Component	
	1	2
^{238}U	0.981	0.11
^{232}Th	0.925	0.381
^{40}K	0.284	0.959
Ra_{eq}	0.926	0.378
D_R	0.925	0.379
AEDR	0.925	0.379
H_{ex}	0.926	0.378
Variance explained in %	76.05%	23.57%

Fig. 12 — Spatial distribution of ^{238}U and ^{232}Th.

calculated. Table 5 displayed the results of the factor loadings with a varimax rotation, as well as the eigen values and communalities. The results showed that there were two eigen values higher than one and that these two factors could explain over 99.62% of the total variance. Normally, an ordination result was good if the value was 75% or better (Zhang, Lu, Dawson, Shi, & Wang, 2005). As seen from Table 4, the first component (PC1) explained 73.81% of the total variance and loaded heavily on uranium and thorium series. The second component (PC2), was correlated very strongly with potassium and D_R with a high loading value (0.959 and 0.379, respectively), accounting for 23.57% of the total variance. Fig. 10 shows the rotated factor loadings of radiological parameters.

Fig. 10 — Rotated factor loadings of component-1 (76.05%) and component-2 (23.57%).

radiological parameters. Hence this strong relationship shows the all three radionuclides contribute the emission of gamma radiation in all the locations.

4.4. Principal component analysis

Principal component analysis (PCA) was applied to identify variables by applying varimax rotation with Kaiser Normalization. By extracting the eigen values and eigen vectors from the correlation matrix, the number of significant factors and the percent of variance explained by each of them were
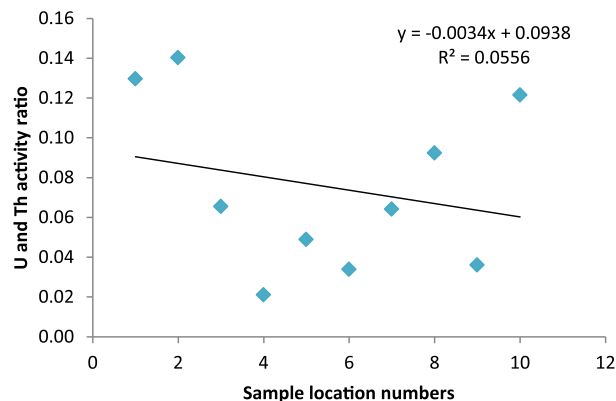
4.5. Cluster analysis

Cluster analysis (CA) is one of multivariate techniques used to identify and classify groups with similar characters in a new group of observations. Each observation in a cluster is most like others in the same cluster. Similarity is a measure of distance between clusters relative to the largest distance between any two individual variables. The zero distance means the clusters are 100% similarity in their sample measurements, whereas the cluster areas are as disparate as the least similar region means similarity of 0%. Cluster analysis was carried out through axes was to identify similar characteristics among natural radio-isotopes and radiological parameters in the sediments.

In CA, the average linkage method along with correlation coefficient distance was applied and the derived dendrogram
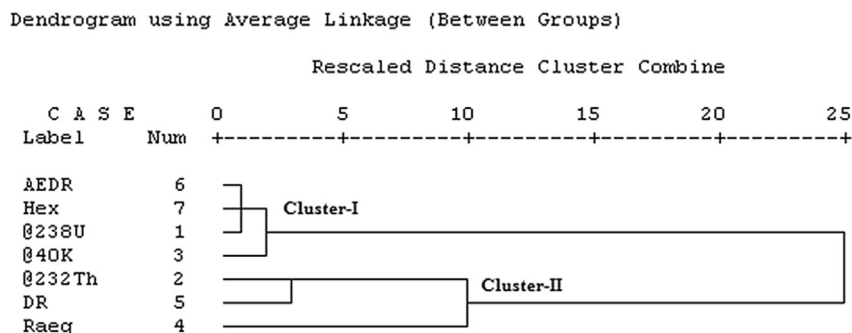

Fig. 11 — Dendrogram shows the clustering of radionuclides.

Table 6 – Activity ratios.

S. no	Location	$^{238}U/^{232}Th$	$^{232}Th/^{238}U$	$^{232}Th/^{40}K$	$^{238}U/^{40}K$
1	Besant Nagar	0.13	7.72	0.99	0.13
2	Thiruvanmiyur	0.14	7.13	0.38	0.05
3	Payanurkuppam (AVM Studio)	0.07	15.26	1.46	0.10
4	Kovalam Creek (Estuary)	0.02	47.44	0.27	0.01
5	Nemilikuppam	0.05	20.45	6.99	0.34
6	Mahabalipuram	0.03	29.50	5.10	0.17
7	Kalpakkam	0.06	15.60	1.31	0.08
8	Periyakuppam	0.09	10.82	0.08	0.01
9	Perumthuravu	0.04	27.73	1.26	0.05
10	Marakanam (Estuary)	0.12	8.23	0.62	0.08
Average		0.08	18.99	1.85	0.10

was shown in Fig. 11. In this dendrogram, all 7 parameters were grouped into two statistically significant clusters. Cluster-I consist of AGDR, H_{ex}, ^{238}U and ^{40}K. Cluster-II consists of ^{232}Th and other radiological parameters distribution, such as D_R and R_{eq}. From this cluster analysis, external hazard index in this studied area due to concentration of ^{238}U and ^{40}K while dose absorbed by the human beings due to high concentration of ^{232}Th.

5. Spatial distributions

The investigation of ^{238}U : ^{232}Th activity ratio calculations revealed that ^{232}Th activity concentrations are seen to be on the average 20 times higher than the ^{238}U activity concentration in the measured sediment samples. Fig. 12 shows the spatial distribution of ^{238}U and ^{232}Th. Thiruvanmiyur showed the highest U/Th ratio (0.14). This indicated that relatively higher amount of ^{232}Th (713.16 Bq kg^{-1}) exist than ^{238}U (35.12 Bq kg^{-1}). This is could be due to the presence of the loamy sediments at Thiruvanmiyur which have relatively high amount of ^{232}Th.

From the other side, Th/U ratios have been calculated and listed in Table 6. The presence of calcium carbonate sediments could be playing an important role for depletion of the ^{232}Th relative to ^{238}U (Mitchell, Mihalynuk, & Heaman, 2002; NCRP, 1976) have mentioned that 0.7–0.4 is the typical range for igneous zircon. All the sediment samples of studied area have Th/U ratio above this range. (Vazquez, Shamberger, & Hammer, 2005) enlarge the previously mentioned range to 0.3–2 for xenolith zircon. The majority of the measured samples have Th/U ratios match with this range. This could be indicated that the present study confirmed highest presence of zircon in the sediments.

6. Conclusion

Average concentrations of natural radionuclides (^{238}U and ^{232}Th) and all calculated radiological parameters are higher than the recommended level. This may be due to the presence of heavy minerals. According to Radiation Protection 112 and UNSCEAR, 2000 report, except external hazard index, all calculated radiological hazard indices are higher than the recommended level. Therefore, the sediments of north east coast of Tamilnadu beaches pose significant radiological

threat to the people living in the area and tourists going to the beaches for recreation or to the sailors and fishermen involved in their activities in the study area.

REFERENCES

Arogunjo, A. M., Farai, I. P., & Fuwape, I. A. (2004). Dose rate assessment of terrestrial gamma radiation in the delta region of Nigeria. *Radiation Protection Dosimetry, 108*, 73–77.

Beretka, J., & Matthew, P. J. (1985). Natural radioactivity of Australian building materials. Industrial wastes and by-products. *Health Physics, 48*, 87–95.

El Mamoney, M. H., & Khater, A. E. M. (2004). Environmental characterization and radio-ecological impacts of non-nuclear industries on the Red Sea coast. *Journal of Environmental Radioactivity, 73*, 151–168.

Facchinelli, A., Sacchi, E., & Mallen, L. (2001). Multivariate statistical GIS-based approach to identify heavy metal sources in soils. *Environmental Pollution, 114*, 313–324.

Groeneveld, R. A., & Meeden, G. (1984). Measuring skewness and kurtosis. *The Statistician, 33*(4), 391–399.

Harb, S. (2008). Natural radioactivity and external gamma radiation exposure at the coastal red sea in Egypt. *Radiation Protection Dosimetry, 130*, 376–384.

ICRP. (1992). (International Commission on Radiological Protection) Protection against radon-222 at home and at work (ICRP Publication 65) *Annals of the ICRP, 23*(2). Pergamon Press, Oxford.

Kannan, V., Rajan, M. P., Iyengar, M. A., & Ramesh, R. (2002). Distribution of natural and anthropogenic radionuclides in soil and beach sand samples of Kalpakkam (India) using hyper pure germanium (HPGe) gamma ray spectrometry. *Applied Radiation and Isotopes, 57*, 109–119.

Khatir, S. A., Ahamed, M. O., El-Khangi, F. A., Nigumi, Y. O., & Holm, E. (1998). Radioactivity levels in the Red Sea coastal environment of Sudan. *Marine Pollution Bulletin, 36*, 19–26.

Mahur, A. K., Kumar, R., Sonkawade, R. G., Sengupta, D., & Prasad, R. (2008). Measurement of natural radioactivity and radon exhalation rate from rock samples of Jaduguda uranium mines and its radiological implications. *Nuclear Instruments and Methods in Physics Research Section B, 266*, 1591—1597.

Mitchell, G., Mihalynuk, L., & Heaman, L. M. (2002). Age of mineralized porphyry at the logtung deposit W-Mo-Bi-Be (Beryl, Aquamarine), Northwest BC, British Columbia geological survey. *Geological Fieldwork, 1*, 35—40.

Mohanty, A. K., Sengupta, D., Das, S. K., Vijayan, V., & Saha, S. K. (2004). Natural radioactivity in the newly discovered high background radiation area on the eastern coast of Orissa, India. *Radiation Measurements, 38*, 153—165.

NCRP. (1976). *Environmental radiation measurement, recommendations of the National Council of Radiat Prot and Meas.* NCRP Report No. 50.

Radhakrishna, A. P., Somashekarappa, H. M., Narayana, Y., & Siddappa, K. (1993). A new natural background radiation area on the southwest coast of India. *Health Physics, 65*, 390—395.

Ramasamy, V., Murugesan, S., & Mullainathan, S. (2004). Gamma ray spectrometric analysis of primordial radionuclides in sediments of Cauvery River in Tamilnadu, India. *Ecologica, 2*, 83—88.

Saad, H. R., & Al-Azmi, D. (2002). Radioactivity concentrations in sediments and their correlation to the coastal structure in Kuwait. *Applied Radiation and Isotopes, 56*, 991—997.

Sheppard, S. C., & Sheppard, M. I. (1988). Modeling estimates of the effect of acid rain on background radiation dose. *Environmental Health Perspectives, 78*, 197—205.

Singh, H. N., Shanker, D., Neelakandan, V. N., & Singh, V. P. (2007). Distribution patterns of natural radioactivity and delineation of anomalous radioactive zones using in situ radiation observations in Southern Tamil Nadu, India. *Journal of Hazardous Materials, 141*, 264—272.

Suresh, G., Ramasamy, V., Meenakshisundaram, V., Venkatachalapathy, R., & Ponnusamy, V. (2011). Influence of mineralogical and heavy metal composition on natural radionuclide concentrations in the river sediments. *Applied Radiation and Isotopes, 69*, 1466—1474.

Tanaskovic, I., Golobocanin, D., & Miljevic, N. (2012). Multivariate statistical analysis of hydrochemical and radiological data of Serbian spa waters. *Journal of Geochemical Exploration, 112*, 226—234.

Taskin, H., Karavus, M., Ay, P., Topuzoglu, A., Hindiroglum, S., & Karahan, G. (2009). Radionuclide concentrations in soil and lifetime cancer risk due to gamma radioactivity in Kirklareli, Turkey. *Journal of Environmental Radioactivity, 100*, 49—53.

UNSCEAR. (2000). *Exposure from natural radiation sources, Annex-B. Sources and effects of ionizing radiation.* United Nations, New York: United Nations Scientific Committee on the Effects of Atomic Radiation.

Uosif, M. A. M., El-Taher, A., & Abbady, G. E. (2008). Radiological significance beach sand used for climate therapy from Safaga, Egypt. *Radiation Protection Dosimetry, 131*, 331—339.

Vazquez, J. A., Shamberger, P. J., & Hammer, J. E. (2005). Timing of extreme magmatic differentiation at Hualalai and Mauna Kea volcanoes from ^{238}U, ^{230}Th and U-Pb dating of zircons from plutonic xenoliths. In *AGU Fall meeting, 5—9 December, 2000, Moscone Center West, San Francisco, CA, USA*.

Zhang, H., Lu, Y., Dawson, R. W., Shi, Y. J., & Wang, T. (2005). Classification and ordination of DDT and HCH in soil samples from the Guanting Reservoir, China. *Chemosphere, 60*, 762—769.